Pol. J. Environ. Stud. Vol. 33, No. 1 (2024), 211-224
DOI: *10.15244/pjoes/171717* ONLINE PUBLICATION DATE: 2023-11-13

Original Research

Investigating the Soil Wind Erosion in the Black Soil Region of Northeast China Based on ^{137}Cs Tracer Method

Hongtao Jiang[1, 2, 3#], Xiaojia Li[1, 2, 3#], Yong Wang[1, 4,*], Chunrong Guo[1, 5,#], Yaowen Chang[6], Ruiping Zhou[1, 2, 3], Yufeng Zhang[1, 2, 3]**

[1]College of Geographical Science, Inner Mongolia Normal University, Hohhot 010022, Inner Mongolia, China
[2]Inner Mongolia Land Use and Regulation Engineering Technology Research Center, Hohhot 010022, Inner Mongolia, China
[3]Laboratory of Mongolian Plateau Environment & Global Change, Hohhot 010022, Inner Mongolia, China
[4]Inner Mongolia Engineering Research Center for Water-saving Agriculture, Hohhot 010022, Inner Mongolia, China
[5]Inner Mongolia Territorial and Space Planning Institute, Hohhot Inner Mongolia, China, Hohhot 010013, Inner Mongolia, China
[6]Jiangsu Key Laboratory of Soil and Water Conservation and Ecological Restoration, Collaborative Innovation Center of Sustainable Forestry in Southern China of Jiangsu Province, Forestry College of Nanjing Forestry University, Nanjing 210037, China

Received: 13 July 2023
Accepted: 31 August 2023

Abstract

Soil wind erosion is one of the critical drivers of land degradation in the black soil region of northeastern China. In this study, ^{137}Cs background value and soil wind erosion rate was studied by using ^{137}Cs nuclide tracing technique in the black soil region of northeastern China, and wind erosion characteristics such as background value and soil erosion rate over the years were clarified, which has guiding significance for soil and water conservation and agricultural sustainable development in the black soil region of northeast China. The mean area activity of the Hilltop area was 1541 Bq·m^{-2}, which was lower than the background value of 1879.7 Bq·m^{-2} in the study area. At the top of the hill, soil erosion occurred to some extent. The ^{137}Cs profile has distributional characteristics that can be divided into three categories. Most of the ^{137}Cs area activity in Hilltop area is evenly distributed in 0-15 cm, and the ^{137}Cs area activity below 15 cm decreased gradually until it disappeared. The spatial difference of wind erosion rate is significant in the study area, mainly between 7.17-10.13 t·hm^{-2}a^{-1}. The average wind erosion rate of hilltops with different tillage quality depths has little difference. The average wind erosion rate is 8.60 t·hm^{-2}a^{-1}, which belongs to mild erosion. However, its erosion rate is higher than the tolerable soil loss of 2 t·hm^{-2}a^{-1} in the black soil

[#]Contributed equally to the work (H.J., X.L., Ch.G.)
*e-mail : wangyonglsx@imnu.edu.cn
**e-mail: guochunrong2022@163.com

region of northeast China. As a result, soil erosion control in the black soil region of northeast China still requires attention.

Keywords: ^{137}Cs tracer, ^{137}Cs background value, soil wind erosion, black soil region of northeastern China

Introduction

As one of the three famous black soil regions in the world [1], the black soil region in Northeast China covers a vast area of arable land with a long history of reclamation. It is an important commercial grain production base and an important crop production area, meeting the food needs of more than 216 million urban residents annually [2-4], and has played an essential role in guaranteeing national food supply [5]. However, due to the exploitation of land resources and farming activities, soil erosion and land degradation has become one of the most significant environmental problems in this region [6]. Soil erosion in the northeastern black soil region has been severe, with an erosion area of 216,000 km^2 [7]. Slope erosion and gully erosion are generally practiced [8-9], which gravely affects agricultural production in the northeastern black soil region and threatens the national agricultural growth and food security [10]. Therefore, it is of great theoretical significance to conduct and strengthen the monitoring and scientific research on soil erosion in the black soil region of Northeast China to protect the black soil resources and to sustain the agricultural development.

Soil wind erosion is the process of erosion, transport and deposition of fine particles and nutrients in the topsoil layer under the action of wind [11]. Being an important type of soil erosion, soil wind erosion is one of the major environmental problems in many countries and regions of the world [12, 13]. In China, wind erosion affects more than half of the country's land area [14, 15]. The land affected by wind erosion in China is mainly distributed in northern areas, and wind erosion in the black soil region of Northeast China accounts for 21-33% of the total erosion [16] and wind erosion is the primary cause of soil thinning and land degradation in arable land in the black soil region of Northeast China. Soil wind erosion poses a serious threat and damage to soil productivity over time, thus causing profound negative impacts on agricultural production and ecological environment [17]. Therefore, accurate prediction of wind erosion and an understanding of its environmental problems are necessary for soil conservation planning and testing of a variety of controls on soil wind erosion in order to maintain sustainable land use.

The erosion pin method [18, 19], wind erosion disk method [20, 21], sand collector method [22, 23], wind tunnel simulation [24, 25], and indirect analysis methods [26] are presently prevalent in the observation and research of wind erosion processes. Due to the intricate and challenging nature of capturing the wind erosion process, previous studies have relied on sand collector or erosion pin methods, which characterize wind erosion conditions using sand transportation rates, but do not provide a direct quantification of the wind erosion rate on a specific plot [27, 28]. Although the wind erosion circle method and the wind erosion disk method provide information on the wind erosion in a given area, it is necessary to conduct further research. This is due to the small size of the instruments used, which raises questions about the representativeness of the observations, and whether the weighing process damages the soil in-situ [29]. The primary objective of utilizing wind tunnel simulation is to examine wind and sand flow structures at specific wind speeds within the field. Nonetheless, it does not simulate diverse complicated wind and sand activities in the field [30]. The indirect analysis approach involves evaluating wind erosion conditions via comparing differences in soil particle compositions before and after wind erosion. However, because of natural erosion, biological processes, and human intervention, the soil undergoes continual changes in particle size composition in its natural state. Therefore, it is challenging to make an accurate comparison of particle size pre- and post-wind erosion. Various models such as WEQ, RWEQ, and WEPS are utilized to estimate wind erosion rates by taking into consideration various factors that impact the wind erosion process. Many of the factors included in the models are obtained empirically from the observation process, and it is difficult to sort out their independence and connections. Verification of the applicability of the tests necessitates observational data [11, 31-33].

The radionuclide ^{137}Cs has been extensively employed to quantify soil erosion [34, 35]. Afshar et al. [36] estimated the rate of soil reformation in western Iran using ^{137}Cs radionuclides and the erosion and deposition rates are 29.8 and 21.8 t·hm^{-2}a^{-1}, respectively. Amini et al. [37] have investigated the amount of sediment of Holocene in Gorgan gulf and southeastern coast of the Caspian Sea. In China, the impact of ^{137}Cs tracer technology on soil erosion has been studied since the 1980s, and the study area has been extended from the Qinghai-Tibetan Plateau region [38-40] to the Yangtze River Basin [41, 42], the Southern Red Loam region [43], the Loess Plateau region [44], the Northwestern Sandy Wind region [45, 46], the Rocky Desertification region [47, 48], and the Northeastern Black Soil region [49, 50], and the land use has involved forested land [51], grassland [25], sandy land [52], cropland [20], and many other land use types. It involves many land use types such as forestland [51], grassland [25], sandy land [52], and cropland [20]. And the study subjects have developed from the beginning of water erosion to the later wind erosion. An important part of these research results is the determination of the background values in the study area, which provides some theoretical basis for future research in this field. While the ^{137}Cs method does not give a reliable estimate of soil erosion caused by non-continuous hydrological events or over the short-term before ^{137}Cs deposition, it is useful for determining soil erosion and accumulation rates on a medium scale (approximately 60 years).

Therefore, this study has two objectives. The initial objective is to collect and analyze the distribution and profile characteristics of the area activity of ^{137}Cs in the northeastern black soil of Hilltop by using the ^{137}Cs tracer method. The second objective is to quantify the soil erosion rate using the mass balance model. This study aims to promote soil and water conservation measures in the region, while also supporting sustainable development in agriculture and forestry in China's black soil region.

Materials and Methods

Study Area

The research area is located in Hebei Watershed (48°50'N-49°10'N, 125°00'E-125°30'E, Fig. 1) within the Heshan Farm, Jiusan Branch, Heilongjiang General Administration of Agriculture and Reclamation, which belongs to the typical black soil area in Northeast China. The climate is cold temperate continental monsoon climate, with obvious seasonal differences, high temperature and rainy in summer, large temperature difference between day and night in autumn and cold and snowy in winter. The average temperature in January is -22.5ºC, the average temperature in July is 20.8ºC, the frost-free period is short, the freezing period is long, and the frozen soil depth is 1.5-2.0 m. The annual average precipitation was 534 mm, mainly from June to August, accounting for 66.6% of the annual precipitation. There is less precipitation in spring, the average precipitation is 60.4 mm. Located at the southern foot of the Lesser Khingan Mountains, this area is a transition zone from the Lesser Khingan Mountains to the Nenjiang Plain. It is a rolling hilly area with a mean slope of 2%. Most of the landforms are high plains and piedmont alluvial plains that intermittently rose and suffered various degrees of cutting during the modern geotectonic movement. The soil is given priority by the typical black soil, and the crop growth period is short, with one ripe year, mainly planting corn, soybean and spring wheat.

The study area demonstrates an average wind speed of 3.13 m·s^{-1}, with winds concentrated mainly in the northwest and southwest. Fig. 2 shows a relatively high frequency of >5 m·s^{-1} and maximum wind. Due to the flat landscape and breezy climate, the black soil is vulnerable to wind erosion.

Sample Collection and Processing

According to the topographical features of the study area, hilltops were selected as the preferred area for arranging sampling points. Although the sampling point itself is situated on a flat hilltop, there are variations in micro-topography across different sampling sites, resulting in depressions in some locations. These, combined with hydraulic factors, lead to abnormal accumulation of ^{137}Cs. Meanwhile, other areas may have small bumps, which accelerate the loss of ^{137}Cs due to hydraulic erosion. Therefore, it is necessary to check the sampling points and remove the anomalies to make the study more accurate. In this study, the Grubbs criterion was used for rejection. This criterion assumes that the observed data follow normal distribution,

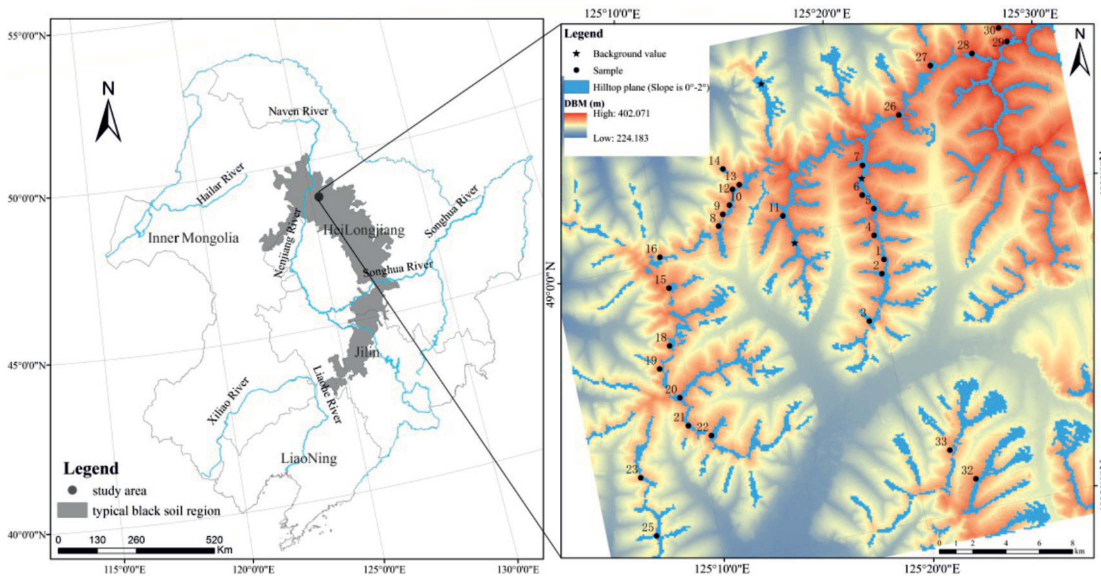

Fig. 1. Location of sampling sites.

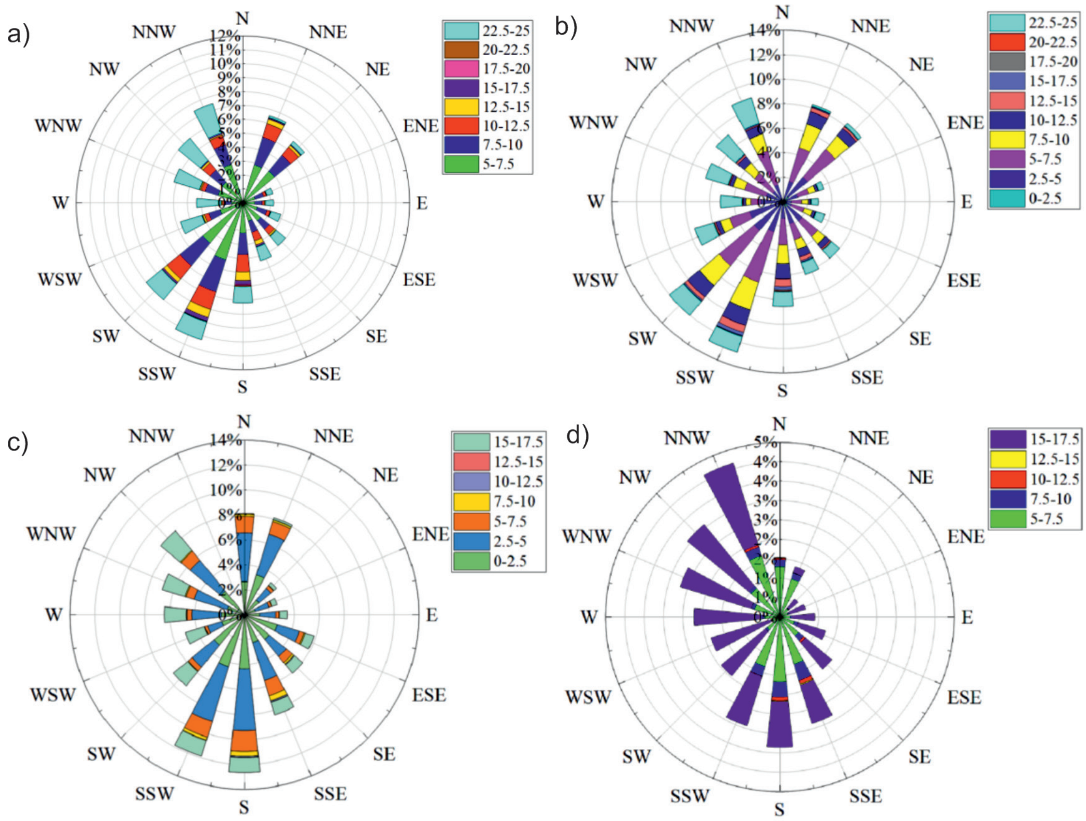

Fig. 2. Wind conditions of study area (m·s^{-1}). a) ≥5 m·s^{-1} wind speed, direction and frequency; b) Maximum wind speed, direction and frequency; c) Mean daily wind speed; d) Mean daily ≥5 m·s^{-1} wind speed.

and the obtained values are arranged in ascending order. In the normal case, data outliers occur under extreme conditions, i.e. minimum or maximum values. Based on this principle, the event hazard rate is selected, and when the measured event is greater than the hazard rate, then the point is considered abnormal. After field investigation, sample points that did not meet the sampling requirements due to topographic features were excluded. Ultimately, 30 hilltops were selected as the ^{137}Cs sampling points for this study. Hilltop the sampling points were all located at the hilltops with slope close to 0, assuming that only wind erosion occurs at these hilltops (Fig. 1). Each hilltop is designed with 9 sampling points, and the hilltop center is designed with one sampling point. The rest of the sample points lie on two mutually perpendicular lines through the center, with an interval of 30 meters and 60 meters on either side of the center point. The first line is perpendicular to the ridge direction, and the second line is parallel to the ridge direction. This results in a total of 9 sample points being fixated at the top of each hill, as illustrated in Fig. 3. ^{137}Cs samples were collected as bulk samples and incremental samples, with 8 bulk samples and 1 incremental sample taken at each hilltops (Fig. 3). ^{137}Cs soil bulk samples are those containing all ^{137}Cs nuclides collected over a certain area. Soil samples were collected from the vertical slope using a root drill with an inner diameter of 8 cm and a height of 15 cm, and soil samples with a soil depth of 30 cm were taken twice. The soil samples were packaged into sample bags and brought back to the laboratory for analysis. ^{137}Cs soil incremental samples are soil samples collected in layers, and the tools used are the same as those used for the bulk samples. The cumulative sampling depth of the incremental samples was 45 cm, with one incremental sample every 5 cm (Fig. 3). The incremental samples were collected to ascertain the specific activity of ^{137}Cs in various soil layers, portraying the distribution pattern of ^{137}Cs in the soil profile. This determination is crucial to establish whether the background value sample points are dependable and if the depth of other bulk samples collected in the same area extends beyond the ^{137}Cs threshold.

Based on the topographic map and Google images of the study area, two ^{137}Cs background sampling sites were selected: sample site 1 was located in the Gaofeng Forest Park between Nenjiang County and Heshan Farm of Jiusan General Bureau of Agriculture and Reclamation, and was a flat pine woodland at the top of the diffuse hill, while sample site 2 and 3 was located in a flat secondary natural woodland between teams 6 and 9 of Heshan Farm, with vegetation types of Mongolian oak and birch. Dead branches and fallen leaves cover the surface, with a cover rate of more than 90%. Underneath the dead branches and fallen leaf layer, there is a complete layer of organic matter.

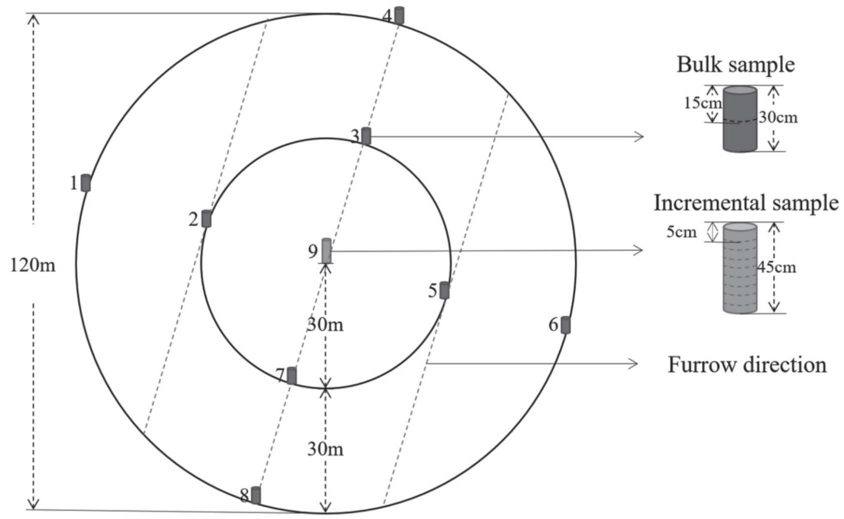

Fig. 3. The layout of the sampling point from top view and sampling method.

Topographic maps and the condition of the soil surface, as well as surveys of the local population, show that the sampled area are flat, with little erosion or accumulation, and have been in a natural state for the past 60 years, undisturbed by human activity. Field investigations found no evidence of human activity. Such sampling sites are consistent with the view of previous scholars that sampling sites of background value should be selected, to the extent possible, in nature reserves, parks, cemeteries and other areas with good natural vegetation, without anthropogenic interference, erosion and accumulation [53-56]. In the first background sample point, 5 holes of whole sample, 2 holes of 5 cm interval layer sample and 1 hole of 2 cm interval layer sample were collected; The other two background value sample points, 2 holes of whole sample and 1 hole of 5 cm interval layer sample were collected. The root drill with an inner diameter of 8 cm and a height of 15 cm was used to collect whole samples and stratified samples, and the sampling depth of both whole samples and stratified samples was 30 cm.

After air-drying naturally, the soil samples were ground and passed through a 2 mm sieve, and the fraction larger than 2 mm was weighed, while the fraction smaller than 2 mm was weighed and boxed for determination of activity. The ^{137}Cs activity of soil samples was measured in the Environmental Radionuclide Laboratory of the State Key Laboratory of Surface Processes and Resource Ecology of Beijing Normal University. The measurement instrument was a coaxial high-purity germanium γ detector (GMX50P4N from ORTEC, USA), and the detector was equipped with a digital multi-channel spectrometer model DSPEC-ji-2.0.

Determination of ^{137}Cs Sample Activity

The commonly used method for measuring the activity of ^{137}Cs is to measure the net area of the full absorption peak of a characteristic γ-ray of a nuclide within a certain time, and then based on the probability of emission of the γ-ray and the detection of the full absorption peak to the activity value of the nuclide, and then divided by the mass of the sample, we can find the specific activity of the nuclide. In this study, the relative comparison measurement method was used. The calculation formula is as follows:

$$A = C_e \frac{A_S F_1}{F_2 T m e^{-\lambda \Delta t}} \tag{1}$$

$$C_e = \frac{A'}{a_s} \tag{2}$$

$$F_1 = \frac{\lambda T_c}{1 - e^{-\lambda T_c}} \tag{3}$$

Where A is the specific activity of the nuclide (Bq/kg), C_e is the scale factor, A' is the activity of the source nuclide (Bq), a_s is the selected one or several weighted (generally weighted by the probability of emission) net area count rate of the characteristic full-energy peak (s^{-1}), A_s represents the net area of the characteristic peak of the nuclide obtained from the beginning to the end of the measurement sample, F_2 is the sample self-absorption with respect to the scale source γ correction factor, F_2 = 1 if the sample density and the density of the scale source are the same or similar; T is the sample measurement activity time (s), m is the mass of the measured sample (kg), Δt is the nuclide decay time, i.e., the time interval (s) between the sampling moment and the sample measurement moment, λ is the radionuclide decay constant (s^{-1}), and F_1 denotes the decay correction factor during the sample measurement if the half-life of the analyzed nuclide is greater than 100 compared to the time of sample measurement, F_1 = 1; T_c is the actual time (s) of the measured sample.

Soil Erosion Rate Computation

Since the introduction of ^{137}Cs tracer technology to the field of soil erosion research, researchers have established numerous theoretical models [57-62]. In order to obtain a more reliable rate of wind erosion, two Mass balance models were chosen in the present study, one of which is the model of Walling and He [63], and the other, the Zhang 's model [64].

Walling and He's mass balance model (II):

$$\frac{dA(t)}{dt} = (1-\tau)\ I\ (t) - \left(\lambda + P\frac{R}{d_m}\right)A(t) \quad (4)$$

Where τ indicates the percentage of newly deposited ^{137}Cs eroded off portion before it is mixed into the tillage layer, which is chosen as 0.5 in this study; P is the particle size correction factor, the ratio of ^{137}Cs concentration in the mobile deposited portion of soil to ^{137}Cs activity in erosion-migrated soil. This model takes into account the interannual variation of ^{137}Cs deposition flux, the loss of newly deposited ^{137}Cs before they are fully mixed with the cultivated soil, and the sorting nature of erosion. As a result, the accuracy of this model is high. Since the mass balance model not only provides a theoretical analysis of the soil erosion mechanism, but also considers the influence of the interannual variation of the settling fraction of ^{137}Cs during settlement on the estimation of soil erosion rate, the soil erosion rate obtained by applying the mass balance model is relatively accurate, making it one of the most widely used theoretical models.

Zhang's Mass balance model:

$$A = A_0\left(1-\frac{\Delta H}{H}\right)^{N-1963}$$

where A indicates Area activity of ^{137}Cs at the erosion sampling location (Bq m^{-2}); A_0 is ^{137}Cs background value (Bq m^{-2}); H is the plow layer thickness (cm); ΔH is thickness of annual soil loss (cm); and N indicates The year of sampling. The model is primarily based on the settlement of ^{137}Cs during the 1950s and 1970s, with ^{137}Cs being the largest settlement in 1963 and a similar one before and after 1963. Then all ^{137}Cs are assumed to have settled by 1963 and the advantage of this model is that it has fewer parameters and is easily estimated.

In this study, the mass depth data were obtained by multiplying the tillage depth and the capacity weight based on the buried depth of ^{137}Cs, together with the capacity weight data of the surface soil. All the hilltops were selected with a surface soil capacity of 1.2 g·cm^{-3}, and the tillage depth was divided into two types according to the distribution characteristics: one was 20 cm with a mass depth of 240 kg·m^{-2}; the other was 25 cm with a mass depth of 300 kg m^{-2}, in total 12 hilltops including 6, 10, 12, 13, 14, 16, 22, 23, 27, 28, 29, 30, and the tillage quality depth of the remaining 18 hilltops is 300·kg m^{-2}.

Results

^{137}Cs Background Values

Determination of the background value is a prerequisite for the calculation of soil erosion rate by ^{137}Cs tracer method. Fig. 4 shows the distribution characteristics of the three background profiles in the area, the total activity of background sample point A, background sample point B and background sample point C are 1593 Bq·m^{-2}, 1671 Bq·m^{-2} and 2090 Bq·m^{-2} respectively, and the background value of the study area is 1879.7 Bq·m^{-2} based on the average activity of the full background sample and layer sample, and the model simulation value is 1911.2 Bq·m^{-2}. The measured value is basically the same as the model simulated value. As shown in Fig. 4, the background sample points A and B have a layer every 5 cm, and the background sample point C has a layer of 2 cm. The background layer samples of sample point A and sample point B show an evident decreasing number distribution from 0 to 25 cm, while the background sample point C exhibits a peak activity value at 2-4 cm, but also shows an overall exponentially decreasing distribution.

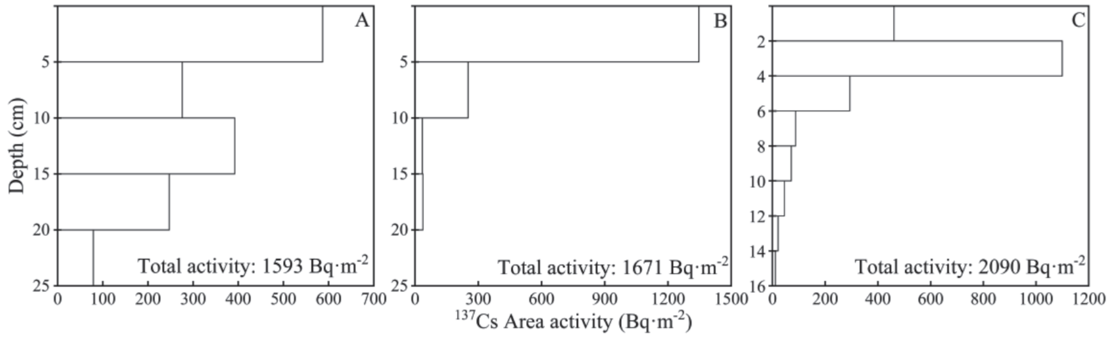

Fig. 4. The area activity profiles of ^{137}Cs in the background points (A and B are 5 cm layer samples, C is 2 cm layer sample).

^{137}Cs Profile Distribution

The ^{137}Cs profile activity characteristics are the basis for determining whether the sampling effort can reach the ^{137}Cs buried depth, and for verifying whether the sampling effort is reasonable and whether the next sampling effort is necessary. In addition, the ^{137}Cs profile distribution characteristics also provide the basis for the determination of the tillage depth parameters required in the model calculation process. Based on the area activity characteristics of 30 layered ^{137}Cs samples at the hilltops, the ^{137}Cs profile distribution in this study can be categorized into three forms: 1) the uniform distribution of ^{137}Cs in the surface layer of the cultivated land, and most of the study area belong to this type of distribution, which is consistent with the profile distribution of ^{137}Cs in cultivated land; 2) uniform in the upper layer at a certain depth, and the content of ^{137}Cs in the soil increases rapidly in the next layer, which is probably due to the deep plowing of the local soil at about 40 cm by large machinery 20 to 30 years ago, and the plowing depth has not reached 40 cm since the deep plowing, after which the ^{137}Cs in the surface layer gradually decreases at a certain distance with the erosion phenomenon, while the ^{137}Cs in the bottom layer basically remains unchanged after the deep plowing, thus producing such a profile distribution characteristic; and 3) exponentially decreasing with the deepening of depth, which may be related to the years of reclamation of Hilltop, and the later reclamation leads to higher ^{137}Cs distribution in the surface layer than in the lower layer, for example, the profile distribution features of ^{137}Cs at the hilltops of 13, 17 and 20 (Fig. 5).

As shown in Table 1, the total activity at each site was concentrated between 1000-2500 Bq·m^{-2}, with the maximum value of 2531 Bq·m^{-2} and the minimum value of 990 Bq·m^{-2}. The average total activity was 1613.3 Bq·m^{-2}, and the average ^{137}Cs profile at the hilltops in Fig. 6 showed a uniform distribution from 0 to 15 cm. After 15 cm, the ^{137}Cs content gradually decreased

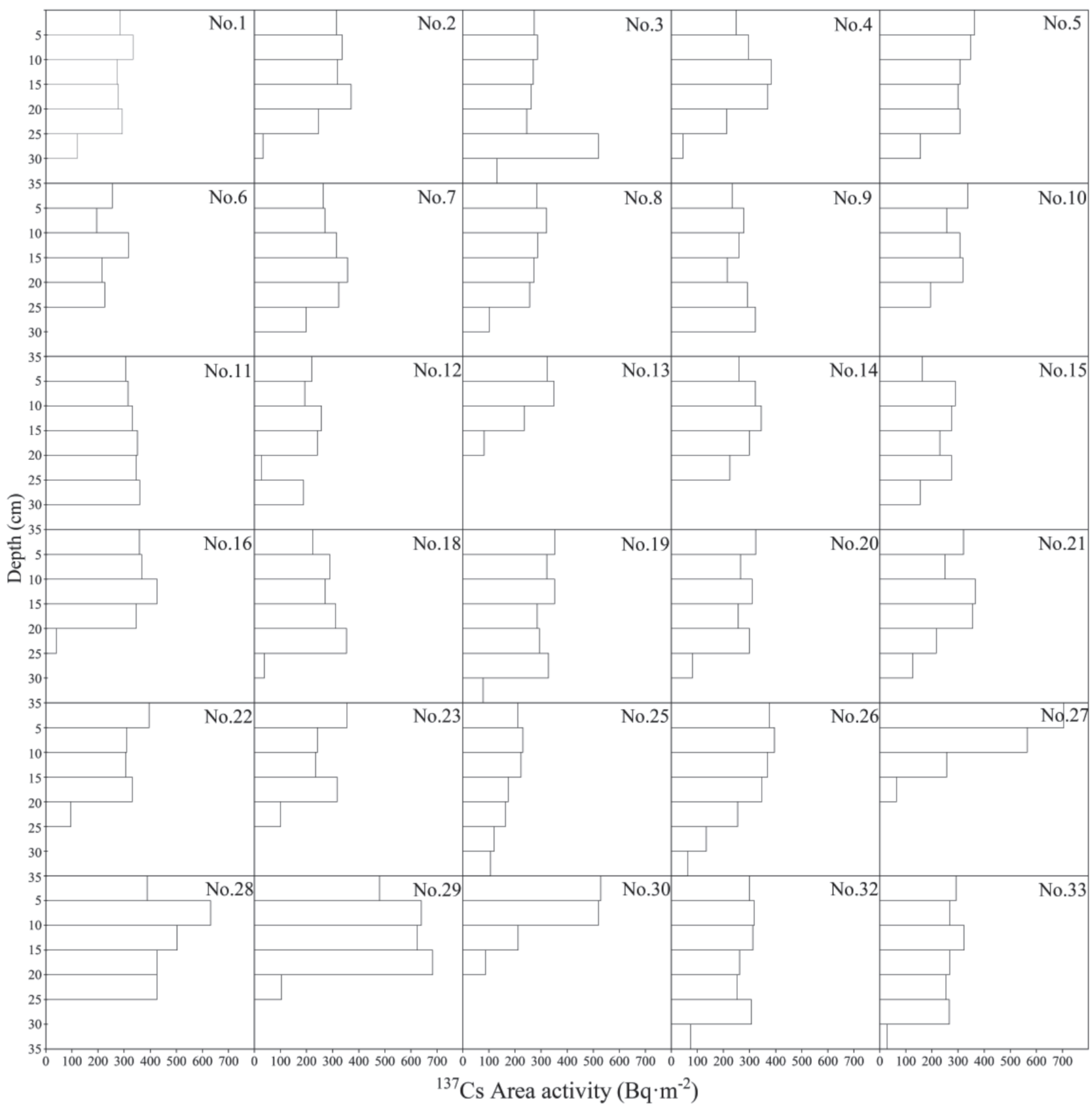

Fig. 5. The area activity profile of ^{137}Cs in the soil layer at each sample site.

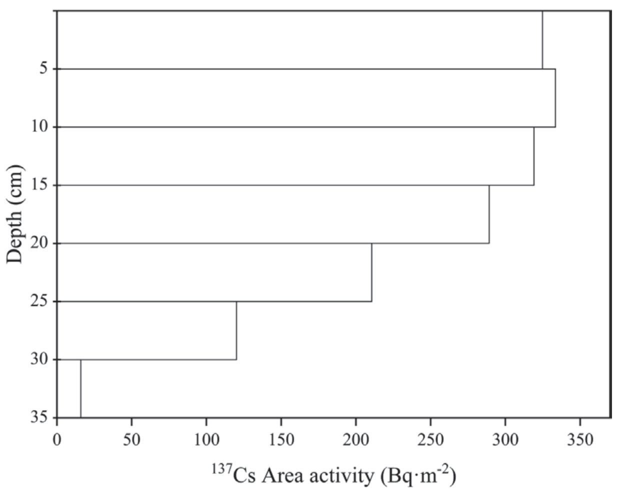

Fig. 6. Average profile characteristics of ^{137}Cs area activity.

until it disappeared with the increase of depth. Most of the sample sites disappeared when the ^{137}Cs content reached 30 cm depth, but the sample sites No. 3, No. 19, No. 25, No. 26, No. 32 and No. 33 still exhibited ^{137}Cs at 30-35 cm.

Erosion Rate Characteristics of the Studied Area

Based on the Grubbs criterion, we have excluded 24 samples from the 270 collected from 30 hilltops due to their outlier status. These samples included eight full ^{137}Cs samples and one ^{137}Cs layer sample. After removing the outliers, the average area activity of the remaining samples indicates that the 30 Hilltops in our study area have an activity of 1541 Bq·m^{-2}, which is significantly lower than the background value of 1879.7 Bq·m^{-2}. This suggests that soil erosion has occurred at the hilltops. The area activity of ^{137}Cs between the hilltops did not vary significantly, ranging from 1328 Bq·m-2 to 1764 Bq·m^{-2}, with a mean value of 1548 Bq·m^{-2}, which closely resembles the median value. These results indicate that the area activity of ^{137}Cs conforms to a normal distribution, with a standard deviation of 115 and a coefficient of variation of 7. The study found that 47% of the samples were small. The mean error at a 95% confidence level was only 43 Bq·m^{-2}, which suggests that there was no significant difference in the mean area activity of ^{137}Cs across all sampling sites in the study area.

The erosion rate computed by two Mass balance models was averaged as the erosion rate value of the sample points to give a relatively reliable erosion rate. The wind erosion rates of the two types of hilltops are shown in Fig. 7, where the average wind erosion rate of 300 kg·m^{-2} is 9.05 t·hm^{-2}a^{-1} and the average wind erosion rate of 240 kg·m^{-2} is 8.30 t·hm^{-2}a^{-1}. The difference in the average wind erosion rate between the two types of hilltops was small, and the one with a tillage mass depth of 240 kg·m^{-2} was slightly larger than the one with a tillage mass depth of 300 kg·m^{-2}. The mean wind erosion rate for all sample sites was 8.60 t·hm^{-2}a^{-1} with a median of 9.01 t·hm^{-2}a^{-1}, and the mean and median values were very similar. The difference between the maximum and minimum

Table 1. Area activity of 137Cs in stratified samples at each hilltop.

Index	Area activity of ^{137}Cs in each soil layer (Bq·m^{-2})							Sum
	0-5	5-10	10-15	15-20	20-25	25-30	30-35	
1	286	334	275	278	293	120	0	1586
2	315	337	318	371	245	33	0	1619
3	274	286	270	262	245	520	130	1987
4	248	296	383	370	212	44	0	1553
5	363	348	307	300	307	156	0	1781
6	254	195	317	215	226	0	0	1207
7	264	270	315	357	324	199	0	1729
8	283	321	287	273	256	102	0	1522
9	233	278	260	215	291	323	0	1600
10	338	256	307	318	194	0	0	1413
11	306	315	332	351	346	360	0	2010
12	221	193	257	241	28	189	0	1129
13	324	350	235	81	0	0	0	990
14	259	323	345	299	225	0	0	1451
15	164	289	276	230	275	154	0	1388

Table 1. Continued.

16	359	367	426	346	41	0	0	1539
18	225	289	272	312	353	39	0	1490
19	352	322	351	285	293	328	78	2009
20	324	265	310	257	300	81	0	1537
21	321	251	366	356	216	127	0	1637
22	396	310	307	331	96	0	0	1440
23	355	242	235	317	101	0	0	1250
25	210	230	223	174	163	120	106	1226
26	375	396	369	347	254	134	64	1939
27	706	565	256	64	0	0	0	1591
28	388	632	503	425	425	0	0	2373
29	480	640	624	683	104	0	0	2531
30	529	520	212	86	0	0	0	1347
32	300	318	313	262	252	307	75	1827
33	292	267	323	267	254	266	28	1697

values is 8.9 t·hm^{-2}a^{-1} with a standard deviation of 3.82 and a coefficient of variation of 44.4%. The wind erosion rate in the study area still varies greatly geographically, and the wind erosion rate in the study area is mainly between 7.17 and 11.03 t·hm^{-2}a^{-1}, but the wind erosion rate error is ±0.70 t·hm^{-2}a^{-1} at the 95% confidence level, indicating that the wind erosion level is exactly around 8-12 t·hm^{-2}a^{-1} (Fig. 8, Table 2). The relationship between erosion rates calculated by two Mass balance models is shown in (Fig. 9).

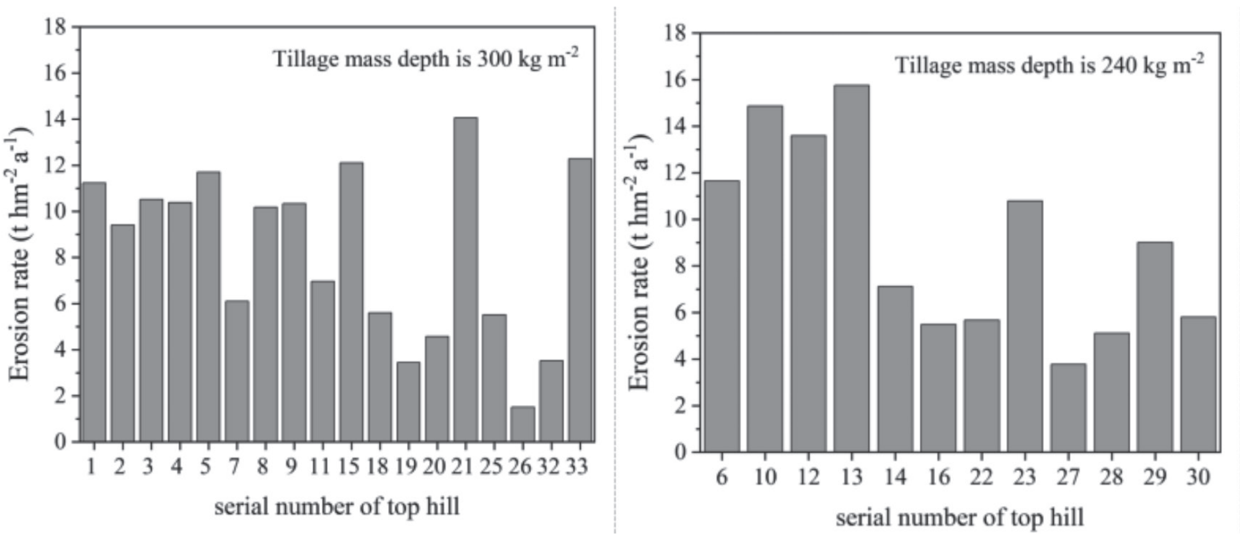

Fig. 7. Erosion rate of hilltop with different tillage quality depth.

Table 2. Statistics of area activity and soil wind erosion rate at sampling sites.

	Mean	Median	Minimum	Maximum	Standard deviation	Coefficient of variation (%)	Confidence level (95%)
Area activity (Bq·m^{-2})	1541	1548	1328	1764	115	7.47	42.98
Erosion rate (t·hm^{-2}a^{-1})	8.60	9.01	1.51	15.75	3.82	44.40	0.70

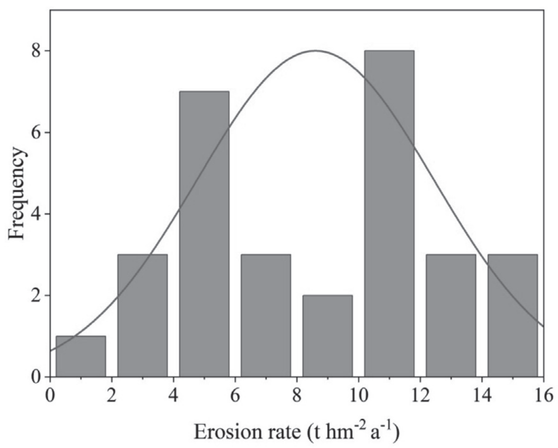

Fig. 8. Histogram of the frequency distribution of the erosion rate of the hilltop.

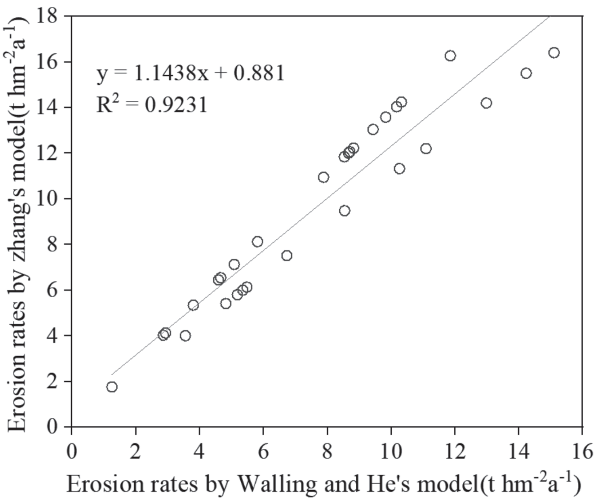

Fig. 9. Relation Diagram of Erosion Rate Calculated by Different Mass balance Models.

Discussion

From the study's findings, the background value in this study area was found to be 1879.7 Bq·m^{-2}, which is similar to the background values measured by Qi et al. [65] in the flat woodland of Nenjiang County, Heilongjiang Province and Hu et al. [66]. In the central-eastern part of Inner Mongolia. At the same time, the background values are relatively high compared to those measured by Fang et al. [67] in agricultural land at the hilltops, Dehui City, Jilin Province, and low compared to those measured by Yan et al. [68] (Table 3), but the differences are not significant, which may be due to the micro topographic differences in the specific selection of background sampling sites and testing error of the probe of high purity germanium from γ-energy spectrometer, which is used to determine ^{137}Cs activity [69]. It should be noted that the background sample of Yan's study was taken from the grassland, which is prone to the movement and deposition of soil particles [68]. Given that the sampling site's location at the top of the forest park, the forest belt's width measuring several hundred meters, and the saturation path of the sand-carrying wind being close to exhaustion, wind erosion or accumulation is unlike to occur at this site. Moreover, wind and sand movement mainly take place near the surface. On the other hand, the simulated value of 1911.2 Bq·m^{-2} calculated by the model of this study is basically the same as the measured background value, and in summary, the background value of 1879.7 Bq·m^{-2} determined in this study is reliable.

According to Adrian Chappell [70], Yan et al. [68] suggested that correction of the ^{137}Cs specific activity of background profiles is necessary in wind erosion areas to achieve accurate and dependable background values. This is the primary rationale for collecting layer samples and analyzing the characteristics of ^{137}Cs area activity profiles in this study. In this study, we discovered that the distribution of profile samples of ^{137}Cs in the background layer did not adhere to the standard exponential curve of ^{137}Cs activity decreasing with depth, Instead, we observed exceptionally high values of 10-51 cm at sample point A and 2-4 cm at sample point C, which confirms that simulating the background value with the standard exponential form of ^{137}Cs profile distribution curve may overestimate the surface ^{137}Cs activity. Therefore, we cannot use the exponential form curve to correct the ^{137}Cs profile distribution curve. Zhang et al. [71] and Li et al. [72] also found that the distribution characteristics of ^{137}Cs background layer samples in the surface layer did not exactly follow the standard exponential form, and the ^{137}Cs activity profile characteristics showed a spike-shaped curve

Table 3. Statistics of related studies on background values of ^{137}Cs in the Northeast (Bq·m^{-2}).

Study area	Land use	Measured values	Sampling year	Measured values after correction	Author
Jiutai City, Jilin Province (44°6′N, 125°58′E)	Wide valley gentle terrace scrub	2463.4	2003	2003.2	Yan et al. [49]
Dehui City, Jilin Province (44°43′N, 125°51.6′E)	Hilltop farmland	2232.7	2002	1774.4	Fang et al. [48]
Nengjiang County, Heilongjiang Province (49°9′N, 125°13′E)	Flat woodland	2216.7	2005	1887.4	Qi et al. [46]

in the surface layer 2-4 cm, which was consistent with the ^{137}Cs profile distribution characteristics of sample site C in this study.

When collecting soil samples, it is necessary to ensure that ^{137}Cs in each sample site are completely captured in the soil profile, i.e., the sampling depth of ^{137}Cs is required to be larger than the buried depth of ^{137}Cs. In this study, stratified samples were collected from each hilltop and the accumulated depth of stratified samples was 45 cm. However, the buried depth of ^{137}Cs in arable land is about 30 cm above the surface. The depth of tillage is limited to a certain level, generally about 20 cm. In the black soil region of Northeast China, the land is generally owned by farms collectively, and the land area is vast. In the planting season in spring and plowing season in autumn, large machinery is used, and the plowing depth is deeper than the humans and animals, with a depth of about 25-30 cm. As a result, a sampling depth of 45 cm is suitable for our study, guaranteeing the complete collection of ^{137}Cs in the soil profile. In this study, the analysis of ^{137}Cs stratified samples at each hilltops revealed that the profiles of most of the layers were uniformly distributed in the surface layer, which also confirmed the history of mechanical deep tillage and deep plowing in Northeast China.

The mean wind erosion rate in this study area was 8.60 $t \cdot hm^{-2} a^{-1}$ by the ^{137}Cs method, with an overall distribution between 7.17-10.03 $t \cdot hm^{-2} a^{-1}$, which is consistent with the results of Wang et al. [73] of wind erosion rates of 6.31-11.55 $t \cdot hm^{-2} a^{-1}$ at the tops of two gently sloping hilltops in the black soil region of Northeast China. This result is very close to Wei's measurement of erosion rate ≤8.4t $hm^{-2} a^{-1}$ using the ^{137}Cs method on a flat mountaintop near the study area [74], Due to the fact that the black soil area in Northeast China has always been considered to be dominated by water erosion and freeze-thaw erosion, the ^{137}Cs method is mainly used to trace erosion at the slope and watershed scales in this area [48, 49]. The ^{137}Cs method is rarely used to directly track wind erosion in mountaintop study areas. Therefore, we compare and analyzed the wind erosion rates of other methods in the study area. The result is slightly higher than the 3.63 t $hm^{-2} a^{-1}$ measured by Wang (2020) using the sand collector method [75]. The possible reason for the slightly lower observed wind erosion rate is that the wind resistance caused by the observation instrument reduces the collection efficiency of the sand collector. Overall, this also indicates that soil erosion in the study area has not been improved in recent years. Although soil erosion in the study area is mild, the erosion rate exceeds the tolerable soil loss of 2 $t \cdot hm^{-2} a^{-1}$ in the northeastern black soil region [76]. The wind erosion rates of 11.8-22.4 $t \cdot hm^{-2} a^{-1}$ of farmland in the Qinghai Gonghe Basin using the ^{137}Cs method by Yan et al. [77], 3 $t \cdot hm^{-2} a^{-1}$ of plowed and tilled land in Zhangbei County, Hebei Province using wind erosion discs by Wang et al.[78], and 4.9 $t \cdot hm^{-2} a^{-1}$ of tilled land in Wuchuan County, Inner Mongolia using the wind erosion circle method by Gao et al. [79], and the results of this study were in the same order of magnitude as those of the above scholars. Some scholars used wind erosion models (RWEQ, WEPS) in grasslands in northern China [80], and the Yellow River Basin [33], and obtained similar conclusions. In addition, the wind erosion rate in this study is roughly 20-30% of the overall erosion rate when compared with the total erosion modulus (2000-3500 t km^{-2} a^{-1}) in the recent black soil area [81, 82]. It can be seen from the above studies that wind erosion is still a very important mode of erosion in the Northeast black soil zone, although the majority of the wind erosion in the farmland in northern China is mild.

According to the activity profile characteristics of ^{137}Cs area in this study, most of the sample sites in this study area disappeared when the ^{137}Cs content reached 30 cm in depth, and some sample sites still had less ^{137}Cs at 30-35 cm. To express the profile distribution pattern of ^{137}Cs in the sample sites and its indicative meaning more accurately, the sampling depth should be appropriately increased in the future studies.

Conclusions

In this study, the ^{137}Cs tracer method was utilized to investigate soil erosion traits in the black soil region of Northeast China. The wind erosion traits, including background values and soil erosion rates over the years, were elucidated. These findings have significant implications for agricultural sustainable development and soil and water conservation in Northeast China's black soil region. The primary conclusions are outlined below:

(1) The average area activity of 30 Hilltop in the study area was 1541 $Bq \cdot m^{-2}$, which was significantly lower than the background value of 1879.7 $Bq \cdot m^{-2}$, indicating that a certain degree of soil erosion had occurred at the hilltop in the study area. The distribution characteristics of ^{137}Cs profile are in three forms. Most of the ^{137}Cs area activity is evenly distributed in the surface layer, the second is evenly distributed in a certain depth in the upper layer, and the content of ^{137}Cs increases rapidly in the next soil layer, and the third is in the form of exponential decline with the deepening of depth. The average ^{137}Cs profile distribution at the hilltop in the study area is relatively uniform from 0 to 15 cm, and the activity of each layer is about 325 $Bq \cdot m^{-2}$. The ^{137}Cs content gradually decreases and disappears with the increase of depth after 15 cm.

(2) The average wind erosion rates at 300 $kg \cdot m^{-2}$ and 240 $kg \cdot m^{-2}$ tillage mass depths were 9.05 $t \cdot hm^{-2} a^{-1}$ and 8.30 $t \cdot hm^{-2} a^{-1}$, respectively, and the difference in average wind erosion rate between the two tillage mass depths was small. The average wind erosion rate of all samples is 9.01 $t \cdot hm^{-2} a^{-1}$, and the coefficient of variation is 44.4%. The regional difference of wind erosion rate in the study area is large. The wind erosion rate in the study area is mainly between 4 and 12 $t \cdot hm^{-2} a^{-1}$, which

is mild erosion. However, its erosion rate is higher than the tolerable soil loss 2 t·hm^{-2}a^{-1} in the black soil region of northeast China. Therefore, soil erosion control in the black soil region of northeast China should be paid more attention.

Acknowledgments

This research was funded by the Inner Mongolia Autonomous Region Major Science and Technology Program and the Inner Mongolia Autonomous Region Natural Science Foundation: Sub-theme of the Inner Mongolia Autonomous Region Major Science and Technology Program Project "Research on the Soil Evolution and Regulation Mechanism of Coal Resource Development in the Wind-Damaged Areas" (ZZDZX2018058) and Integration of ecological restoration and management technology in Inner Mongolia Section of the Yellow River Basin based on water demand threshold (2021GG0367).; Project of Natural Science Foundation of Inner Mongolia Autonomous Region, "Research on the mechanism of vegetation-hydrological process mutual feedback and two-way coupling model in the Inner Mongolia section of the Yellow River Basin" (2023ZD21). Conflicts of Interest: The authors declare no conflict of interest.

Conflicts of Interest

The authors declare no conflict of interest.

References

1. WANG X.K., GU J., LIU G., SHI H.Q. The Influence of Transverse and Longitudinal Ridge Tillage on Soil Erosion and Deposition Cycles for Mollisol Slope. Acta Pedologica Sinica, **59**, 430, **2022** [In Chinese].
2. ZHAO N.B., YANG J.J., ZHAO Y.J., QIN K., YANG Y.C., LI M. Comprehensive Evaluation of Black Soil Quality Based on Aerial Hyperspectral Inversion. Journal of Agricultural Science and Technology, **23**, 88, **2021** [In Chinese].
3. WEN Y., KASIELKE T., LI H., ZEPP H., ZHANG B. A case-study on history and rates of gully erosion in Northeast China. Land Degrad. Dev., **32**, 4254, 2021.
4. WANG B., ZHAO X., WANG X., ZHANG Z., YI L., HU S. Spatial and Temporal Variability of Soil Erosion in the Black Soil Region of Northeast China from 2000 to 2015. Environ Monit Assess, **192**, 370, **2020**.
5. HAN X.Z., LI N. Research Progress of Black Soil in Northeast China. Scientia Geographica Sinica, **38**, 1032, **2018** [In Chinese].
6. AN J., ZHENG F., WANG B. Using ^{137}Cs Technique to Investigate the Spatial Distribution of Erosion and Deposition Regimes for a Small Catchment in the Black Soil Region, Northeast China. Catena, **123**, 243, **2014**.
7. ZHANG G.H., YANG Y., LIU Y.N., WANG Z.Q. Advances and Prospects of Soil Erosion Research in the Black Soil Region of Northeast China. Journal of Soil and Water Conservation, **36**, 1, **2022** [In Chinese].
8. SHEN H.O., WANG D.L., WEN L.L., ZHAO W.T., ZHANG Y. Soil Erosion and Typical Soil and Water Conservation Measures on Hillslopes in the Chinese Mollisol Region. Eurasian Soil Sci, **53**, 1509, **2020**.
9. WANG R., SUN H., YANG J., ZHANG S., FU H., WANG N., LIU Q. Quantitative Evaluation of Gully Erosion Using Multitemporal UA V Data in the Southern Black Soil Region of Northeast China: A Case Study. Remote Sens, **14**, 1479, **2022**.
10. LIU H., ZHANG T., LIU B., LIU G., WILSON G.V. Effects of Gully Erosion and Gully Filling on Soil Depth and Crop Production in the Black Soil Region, Northeast China. Environ. Earth Sci., **68**, 1723, **2013**.
11. WU X., FAN J., SUN L., ZHANG H., XU Y., YAO Y., YAN X., ZHOU J., JIA Y., CHI W. Wind Erosion and Its Ecological Effects on Soil in the Northern Piedmont of the Yinshan Mountains. Ecological Indicators, **128**, 107825, **2021**.
12. BORRELLI P., PANAGOS P., BALLABIO C., LUGATO E., WEYNANTGS M., MONTANARELLA L. Towards a Pan-European assessment of land susceptibility to wind erosion. Land Degradation Development, **27**, 1093, **2016**.
13. WEBER J., KOCOWICZ A., DEBICKA M., JAMROZ E. Changes in soil morphology of Podzols affected by alkaline fly ash blown out from the dumping site of an electric power plant. Soils Sediments, **17**, 1852, **2017**.
14. ZHANG J.Q., ZHANG C.L., CHANG C.P., LIU G. Comparison of wind erosion based on measurements and SWEEP simulation: a case study in Kangbao County, Hebei Province, China. Soil and Tillage Research, **165**, 169, **2017**.
15. MENG Z.J., DANG X.H. Interactive effects of wind speed, vegetation coverage and soil moisture in controlling wind erosion in a temperate desert steppe, Inner Mongolia of China. Journal of Arid Land, **10**, 534, **2018**.
16. WANG H., YANG S., WANG Y., GU Z., XIONG S., HUANG X., SUN M., ZHANG S., GUO, L., CUI, J. Rates and Causes of Black Soil Erosion in Northeast China. CATENA, **214**, 106250, **2022**.
17. LIU X., ZHANG S., ZHANG X., DING G., CRUSE R.M. Soil Erosion Control Practices in Northeast China: A Mini-Review. Soil and Tillage Research, **117**, 44, **2011**.
18. ZHENG S.H., LEI L., TIAN K.L., MA B.Q. Application of ultrasonic chain pin sensor for soil wind erosion monitoring. Bulletin of Soil and Water Conservation, **42**, 124, **2022** [In Chinese].
19. YIN Q.H., XIE S.Y. CAI X.L. Differences of soil erosion between micro-topography and microhabitat in clearcutting site of karst rocky desertification area. Bulletin of Soil and Water Conservation, **39**, 44, **2019** [In Chinese].
20. LIN Y., LI H. P., XIAO B. Influencing Factors of Wind Erosion and Their Quantitative Relationships with Erosion Rate in Black Soil Area of Northeast China. Journal of soil and Water Conservation, **31**, 44, **2017** [In Chinese].
21. LI G.R., LI X.L., LI J.F., ZHU H.L., CHEN W.T., ZHAO J.Y., HU X.S., CUI Y.P., LI C.L. Soil Wind Erosion Law in Ochotona Curzoniae Mound of Alpine Meadow in the Yellow River. Journal of soil and Water Conservation, **33**, 110, **2019** [In Chinese].
22. KANG Y.D., XIA K.W., YANG X.H., HUO W., YANG F., HE Q., ALI M. Analysis of horizontal flux and sand collecting efficiency of sand dust near ground surface based on field observations. Transactions of the Chinese Society of Agricultural Engineering, **33**, 168, **2017** [In Chinese].

23. GUO Q., CHENG C., JIANG H., LIU B., WANG Y. Comparative Rates of Wind and Water Erosion on Typical Farmland at the Northern End of the Loess Plateau, China. Geoderma, **352**, 104, **2019**.
24. LIN X.N. Dust Emission and Transport Characteristics of Soil Erosion by Wind and Its Control over Beijing-Tianjin-Hebei Region. Beijing Forestry University, **2021**.
25. WANG J.T., YU M.H., YANG H.L., WU Q.G., LIU T.H. Soil erodibility of typical plant communities in Ulan Buh Desert, ARID LAND GERGRAPHY, **43**, 1543, **2020** [In Chinese].
26. LI X.N., WA X.Y., ZHAO C.Q., ZHANG W.W., WANG C. Wind erosion prevention effect of strip grass cover in grape planting area of Yanhuai basin. Journal of Arid Land Resources and Environment, **35**, 123, **2021** [In Chinese].
27. WANG R.D., LI Q., CHANG C.P., GUO Z.L., LI J.F., ZHANG C.L., ZOU X.Y., WU Y.S., ZHOU N. Review of Field Measurement Technologies in Soil Wind Erosion. Journal of Desert Research, **39**, 113, **2019** [In Chinese].
28. LIU X., KANG Y., CHEN H., LU H. Application of a High-Precision Aeolian Sand Collector in Field Wind and Sand Surveys. Int. J. Environ. Res. Public Health, **18**, 7393, **2021**.
29. QIN H.L., GAO W.S., MA Y.C., ZHAO P.Y. Effect of standing crop stubble on soil erosion by wind under no-tillage. Transactions of the Chinese Society of Agricultural Engineering, 66, **2008** [In Chinese].
30. DONG Z., LIU X., WANG X., LI F., ZHAO A. Experimental Investigation of the Velocity of a Sand Cloud Blowing over a Sandy Surface. Earth Surf. Process. Landforms, **29**, 343, **2004**.
31. MANDAKH N., TSOGTBAATAR J., DASH D., KHUDULMUR S. Spatial assessment of soil wind erosion using WEQ approach in Mongolia. Journal of Geographical Sciences, **26**, 473. **2016**.
32. ZHANG H.Y., FAN J.W., CAO W., HARRISET WARWICK., LI Y.Z., CHI W.F., WANG S.Z. Response of wind erosion dynamics to climate change and human activity in Inner Mongolia, China during 1990 to 2015. Science of the Total Environment, **639**, 1038, **2018**.
33. CHI W.F., WANG Y.T., LOU Y.X., NA Y., LUO Q.C. Effect of Land Use/Cover Change on Soil Wind Erosion in the Yellow River Basin since the 1990s. Sustainability. **14**, 12930, **2022**.
34. SEKUDEWICZ I., GASIOROWSKI M. Spatial and Vertical Distribution of ^{137}Cs Activity Concentrations in Lake Sediments of Turawa Lake (Poland). Environ Sci Pollut Res Int, **29**, 80882, **2022**.
35. KALKAN S.K., FORKAPIć S., MARKOVIć B.S., GAVRILOV B.M., BIKIT-SCHROEDER K., MRđA D., RADAKOVIć G.M., TOšIć R. Deposition of ^{137}Cs and Precipitation Distribution in Vojvodina, Northern Serbia after the Chernobyl Accident. Chemosphere, **264**, 128471, **2021**.
36. AFSHAR F.A., AYOUBI S., JALALIAN A. Soil Redistribution Rate and Its Relationship with Soil Organic Carbon and Total Nitrogen Using ^{137}Cs Technique in a Cultivated Complex Hillslope in Western Iran. Journal of Environmental Radioactivity, **101**, 606, **2010**.
37. AMINI A., HARAMI R., LAHIJANI H., MAHBOUBI A. Holocene Sedimentation Rate in Gorgan Bay and Adjacent Coasts in Southeast of Caspian Sea. Journal of Basic and Applied scientific Research, **2**, 289, **2012**.
38. YU D., SHA Z.J., WANG Q.G., HU J.F., WANG Z. Distribution characteristics of ^{137}Cs and $^{210}Pb_{es}$ in soil of grassland region in the northeastern of Qinghai - Tibet Plateau. Journal of Arid Land Resources and Environment, **32**, 160, **2018** [In Chinese].
39. WEI M.M., FU S.H., LIU B.Y. Quantitative research of water erosion on the Qinghai-Tibet Plateau. Advances in Earth Science, **36**, 740, **2021** [In Chinese].
40. ZHANG Z.Y., YI P., CHEN P. Soil erosion of Southeastern Qinghai-Tibet Plateau based on 137Cs tracer method. Hubei Agricultural Sciences, **62**, 43, **2023** [In Chinese].
41. PEI Z.L. Using Depression Deposits to Access Sediment Yield from a Karst Catchment in the Three Gorges Reservoir Region, Sichuan Agricultural University, **2020**.
42. JU Z.S., YAN D C., WEN A.B., ZHANG J.B. Sediment delivery ratio and soil erosion quantity on Lingjiaopond small watershed in the Three Gorges Reservoir Region. Journal of Sediment Research, **43**, 67, **2018** [In Chinese].
43. LIU D. Study on Soil Erosion and Soil Fertility under Typical Land Use in Hilly Red Soil Region of South Jiangxi - A Case Study of Nanfeng County, Jiangxi Normal University, **2019**.
44. TSEGAY B.M. Assessment of soil erosion from different land use types using ^{137}Cs technique in Xiashiziwan watershed, Lingbao Loess plateau, Chinese Academy of Agricultural Sciences, **2017**.
45. NIE X.J., GAO S., CHEN Y.L., ZHANG H.B. Characteristics of soil erosion and nutrients evolution under coal mining disturbance in aeolian sand area of Northwest China. Transactions of the Chinese Society of Agricultural Engineering, **34**,127, **2018** [In Chinese].
46. ZHAO L. P. The characteristics and relationship of soil nutrition and ^{137}Cs distribution in the East Junggar region of Xinjiang, Xinjiang University, **2019**.
47. LI Y., LIU Z.Q. Soil erosion and physicochemical properties of different land types in rocky desertification area, Journal of Forest and Environment, **39**, 515, **2019** [In Chinese].
48. YIN Q.H, XIE S.Y., CAI X.L. Differences of soil erosion between micro-topography and microhabitat in clear-cutting site of karst rocky desertification area. Bulletin of Soil and Water Conservation, **39**, 44, **2019** [In Chinese].
49. HE Y.X. Response of Soil Carbon and Nitrogen Changes to Erosion Intensity on Sloping Cropland in the Black Soil Region of Northeast China, Northwest Agriculture and Forestry University, **2022**.
50. WANG X.K., GU J., LIU G., SHI H. Q. The Influence of Transverse and Longitudinal Ridge Tillage on Soil Erosion and Deposition Cycles for Mollisol Slope. Acta Pedologica Sinica, **59**, 430, **2022** [In Chinese].
51. WU Z. ^{137}Cs and $^{210}Pb_{ex}$ tracing of soil erosions on cultivated land and its shelter forest in typical shelter forest areas in North China, Sichuan Agricultural University, **2022**.
52. WANG P., ZHANG P.X., GONG X.J. Tracing Wind Erosion Rates with ^{137}Cs and ^{210}Pb in a Typical Slope on the Southeast Margin of Hunshandake Sandy Land, Inner Mongolia. Chinese Journal of Soil Science, **54**, 569, **2023** [In Chinese].
53. LETTNER H., BOSSEW P. HUBMER A.K. Spatial variability of fallout ^{137}Cs in Austrian alpine regions. Journal of Environmental Radioactivity, **47**, 71, **2000**.
54. GOLOSOV V.N., PANIN A.V., MARKELOV M.V. Chernobyl ^{137}Cs redistribution in the small basin of the Lokna river, Central Russia. Physics and Chemistry of the Earth Part A-Solid Earth and Geodesy, **24**, 881, **1999**.
55. PENNOCK D.J., CORRE M.D. Development and application of landform segmentation procedures. Soil and Tillage Research, **58**, 151, **2001**.

56. ZAPATA F. Handbook for the assessment of soil erosion and sedimentation using environmental radioactivity. Kluwer Academic Publishers, Dordrecht, The Netherlands, 219, **2002**.
57. FENG M.Y., ZHANG X.B., WEN A.B., HE X.B. Assessment of soil losses on cultivated land by using the ^{137}Cs technique in the upper yangtze river basin of China. Soil and Tillage Research, **69**, 99, **2004**. DOI: 10.1016/ S0167-1987(02)00131-9.
58. KACHANOSKI R.G., DE J.E. Predicting the temporal relationship between soil ^{137}Cs and erosion rate. The Journal of Environmental Quality, **13**, 301,**1984**. DOI: 10.2134/jeq1984.00472425001300020025x.
59. WALLING D.E., HE Q. Improved models for estimating soil erosion rates from ^{137}Cs measurements. Journal of Environment Quality, **28**, 611, **1999**. DOI: 10.2134/ jeq1999.00472425002800020027x.
60. YANG H., DU M.Y., ZHAO Q.G., MINAMI K., HATTA T. A quantitative model for estimating mean annual soil loss in cultivated land using ^{137}Cs measurements. Soil Science and Plant Nutrition, **46**, 69, **2000**. DOI: 10.1080/ 00380768.2000.10408763.
61. ZHANG X.B., HIGGITT D.L., WALLING D.E. A preliminary assessment of the potential for using ^{137}Cs to estimate rates of soil erosion in the Loess Plateau of China. International Association of Entific Hydrology Bulletin, **35**, 243, **1991**. DOI: 10.1080/ 02626669009492427.
62. PEGOYEV A.N., FRIDMAN S.D. Vertical profiles of ^{137}Cs in soils. Soviet Soil Science, **8**, 77, **1978**.
63. WALLING D.E., HE Q. Using Fallout Lead-210 Measurements to Estimate Soil Erosion on Cultivated Land. Soil Science Society of America Journal, **63**, 1404, **1999**.
64. LI H., ZHANG X.B., WEN A.B., SH Z.L. Erosion rate of purple soil on a cultivated slope in the three gorges reservoir region using ^{137}Cs Technique. Bulletin of Soil and Water Conservation, **29**, 1, **2009** [In Chinese].
65. QI Y.Q., ZHANG X.B., HE X.B., WEN A.B., FU J.X. ^{137}Cs reference inventories distribution pattern in China. Nuclear Techniques, 42, **2006** [In Chinese].
66. HU Y.F., LIU J.Y., BA T.C.N., ZHEN L. Determination of ^{137}Cs reference inventory in the large scale region: A case study in the central and eastern Inner Mongolia Plateau. Acta Geographica Sinica, **69**, 343, **2014** [In Chinese].
67. FANG H.J., YANG X.M., ZHANG X.P., LIANG A.Z. Study on soil erosion and deposition of black soil on a sloping cultivated land using ^{137}Cs tracer method. Acta Ecologica Sinica, 1376, **2005** [In Chinese].
68. YAN B.X., TANG J. Study on Reference ^{137}Cs Inventory of Black Soil in Northeast China. Journal of Soil and Water Conservation 33, **2004**, [In Chinese].
69. LIU J.Y., WANG M.L. YANG J.J., MIAO C.B. Study on soil erosion in the East Junggar region based on the MCM model and ^{137}Cs. Arid Zone Research, **37**, 1166, **2020** [In Chinese].
70. CHAPPELL A. The Limitations of Using ^{137}Cs for Estimating Soil Redistribution in Semi-Arid Environments. Geomorphology, **29**, 135, **1999**.
71. ZHANG C.L., ZOU X.Y., DONG G.R., ZHANG X.B., QIN Z. Characteristics of soil ^{137}Cs deposition in steppe area. Chinese Science Bulletin, 221, **2002** [In Chinese].
72. LI R.Y., YANG H., ZHAO X.G., TANG X.Y. Application of ^{137}Cs technique to study of soil erosion on Loess plateau region. Soils, 96, **2004** [In Chinese].
73. WANG Y., YANG M.Y., LIU P.L. Contribution partition of water and wind erosion on cultivated slopes in Northeast black soil region of China. Journal of Nuclear Agricultural Sciences, **24**, 790, **2010** [In Chinese].
74. WEI X. Study on spatial differentiation of soil erosion in small watershed in Northeast black soil region. Beijing Normal University, **2007**.
75. WANG L. Hillslope Compound Soil Erosion Processes and Mechanisms under the Interaction of Multiple External Erosive Forces in Chinese Mollisol Region. Northwest Agriculture and Forestry University, **2020**.
76. WANG X.K., GU J., LIU G., SHI H. Q. The Influence of Transverse and Longitudinal Ridge Tillage on Soil Erosion and Deposition Cycles for Mollisol Slope. Acta Pedologica Sinica, **59**, 430, **2022** [In Chinese].
77. YAN P., DONG G.R. Application of the ^{137}Cs technique on wind erosion in the Gonghe basin, Qinghai province. Acta Pedologica Sinica, 497, **2003** [In Chinese].
78. WANG Y.C. Study on soil wind erosion situation of different underlying inecotone between agriculture and animal husbandry in bashang Region of Hebei. Hebei Agricultural University, **2006** [In Chinese].
79. GAO W.S., QIN H.L., ZHAO P.Y. The Effects of Different Planting Modes on Wind Erosion from Cropland in Arid Region of North of Yin Mountain of Inner Mongolia. Research of Soil and Water Conservation, 126, **2005** [In Chinese].
80. LIU T. Spatial and temporal variation of soil conservation services in Jing River Basin and the influencing factors. Xi'an University of Science and Technology. **2021**.
81. LI T., ZHANG H.C., WANG X.Y., CHENG S.L., FANG H.J., LIU G., YUAN W.P. Soil erosion affects variations of soil organic carbon and soil respiration along a slope in Northeast China. Ecological Processes, **8**, 1, **2019**.
82. XU Y.H., QIAO J.X., PAN S.M., HOU X.L., ROOS P., CAO L.G. Plutonium as a tracer for soil erosion assessment in northeast China. Science of The Total Environment, **511**, 176, **2015**.